Supporting information

Metal dependent structural flexibility and intrinsic dynamics in the M$_2$(2,6-ndc)$_2$(dabco) (M = Ni, Cu, Co, Zn) metal-organic frameworks

Nicole Klein,[a] **Herbert C. Hoffmann,**[a, b] **Amandine Cadiau,**[a] **Juergen Getzschmann,**[a] **Martin R. Lohe,**[a] **Silvia Paasch,**[b] **Thomas Heydenreich,**[b] **Karim Adil,**[c] **Irena Senkovska,**[a] **Eike Brunner,**[b*] **and Stefan Kaskel**[a*]

*Prof. Dr. Stefan Kaskel
[a] Department of Inorganic Chemistry
Dresden University of Technology
Bergstr. 66
D-01069 Dresden, Germany
phone: +49-351-46332564
fax: +49-351-46337287
E-mail: Stefan.Kaskel@chemie.tu-dresden.de

*Prof. Dr. Eike Brunner
[b] Bioanalytical Chemistry
Dresden University of Technology
Bergstr. 66
D-01069 Dresden, Germany,
phone: + 49 351 463 32631
Fax: + 49 351 46337188;
E-mail: Eike.Brunner@chemie.tu-dresden.de

[c] Laboratoire des Oxydes et Fluorures,
UMR CNRS 6010, Université du Maine,
Avenue O. Messiaen
72085 Le Mans cedex 05, France
phone: +33 243833352
Fax: +33 243833506,
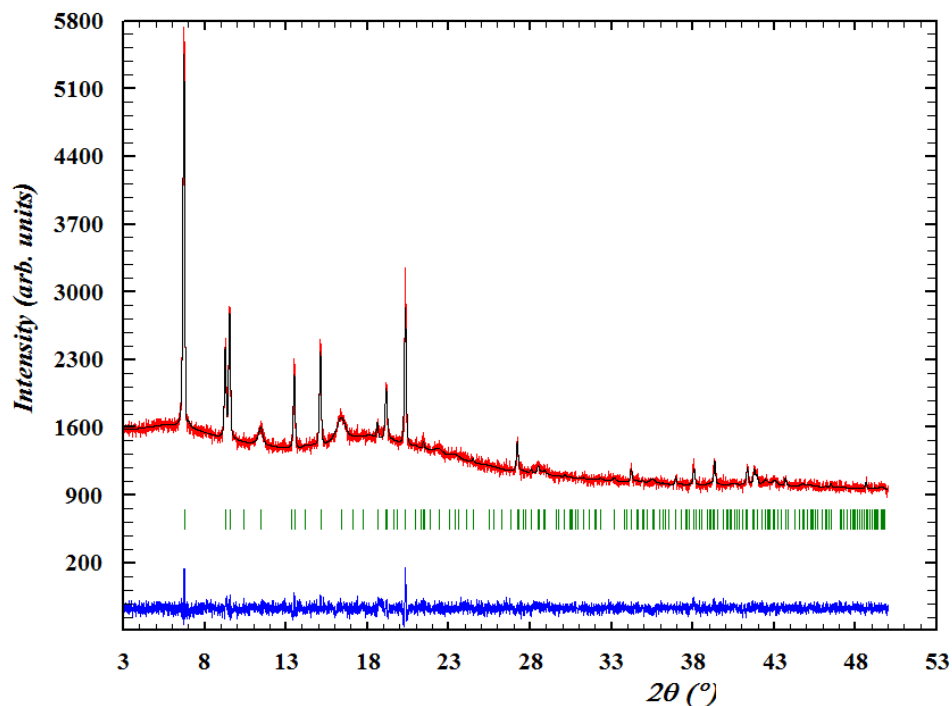E-mail: karim.Adil@univ-lemans.fr

1. Profile refinements

Figure S1: Final profile refinement of DUT-8(Co) (as made): observed (red), calculated (black), and difference (blue) profiles of X-ray diffraction data. Vertical bars (green) are related to the calculated Bragg reflection positions.
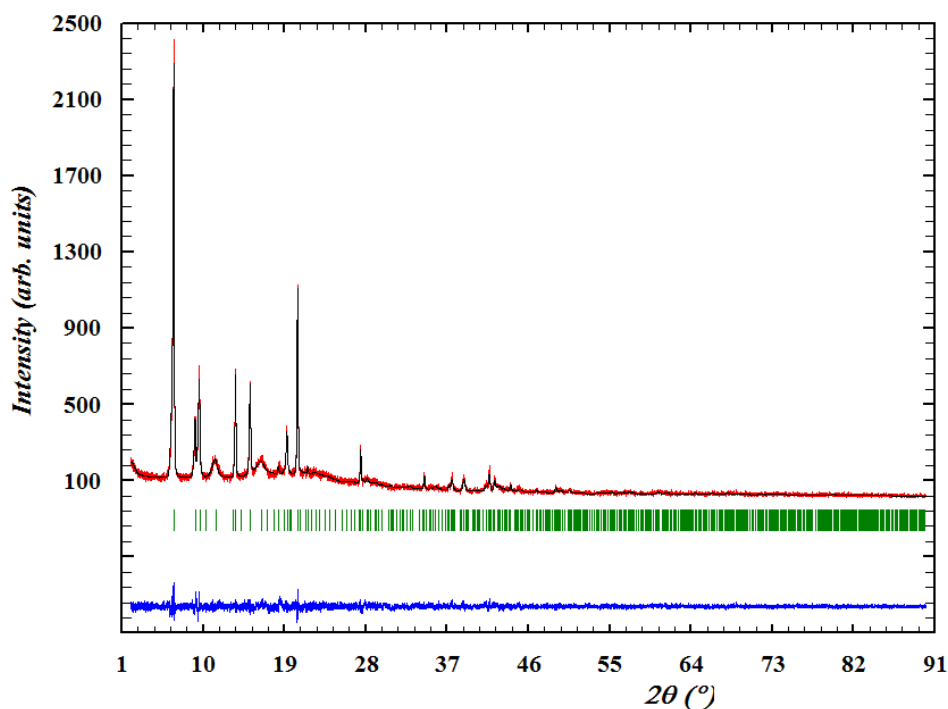

Figure S2: Final profile refinement of DUT-8(Cu) (as made): observed (red), calculated (black), and difference (blue) profiles of X-ray diffraction data. Vertical bars (green) are related to the calculated Bragg reflection positions.
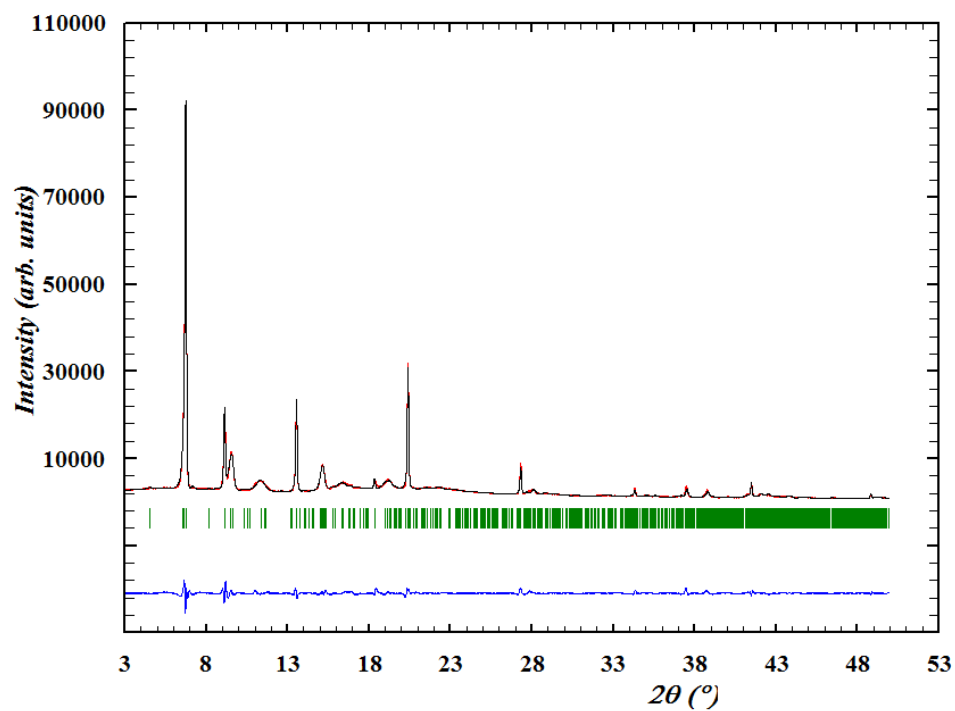
Figure S3: Final profile refinement of DUT-8(Zn) (as made): observed (red), calculated (black), and difference (blue) profiles of X-ray diffraction data. Vertical bars (green) are related to the calculated Bragg reflection positions.

2. Proposed structural flexibility of the DUT-8 series – exemplified for CO_2 adsorption
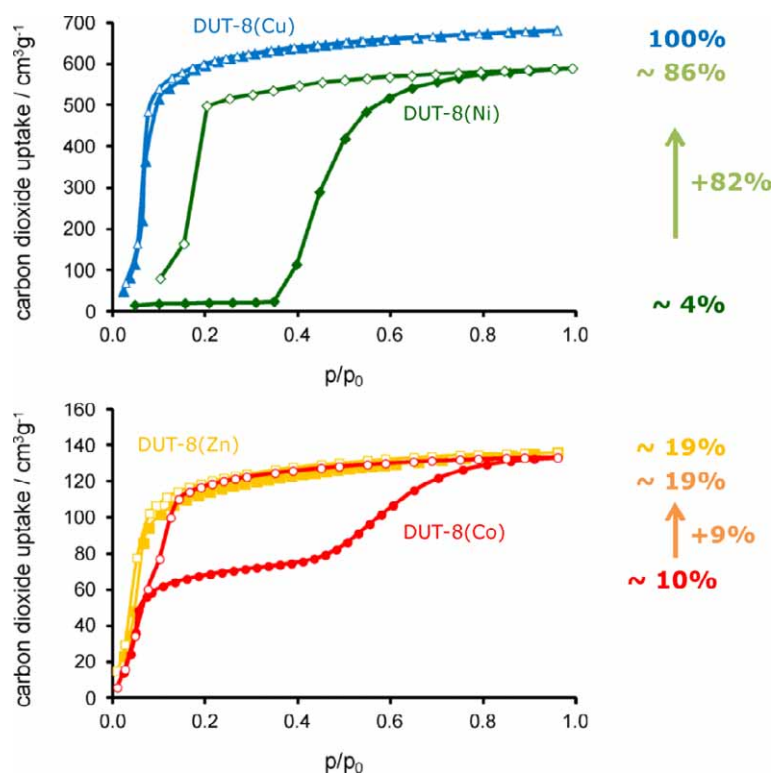

Figure S4: Carbon dioxide adsorption (filled symbols) and desorption (empty symbols) isotherms of DUT-8(Cu) (blue), DUT-8(Ni) (green), DUT-8(Zn) (yellow) and DUT-8(Co) (red), measured at 196 K. The percentaged pore opening is based on the total pore volume of DUT-8(Cu).
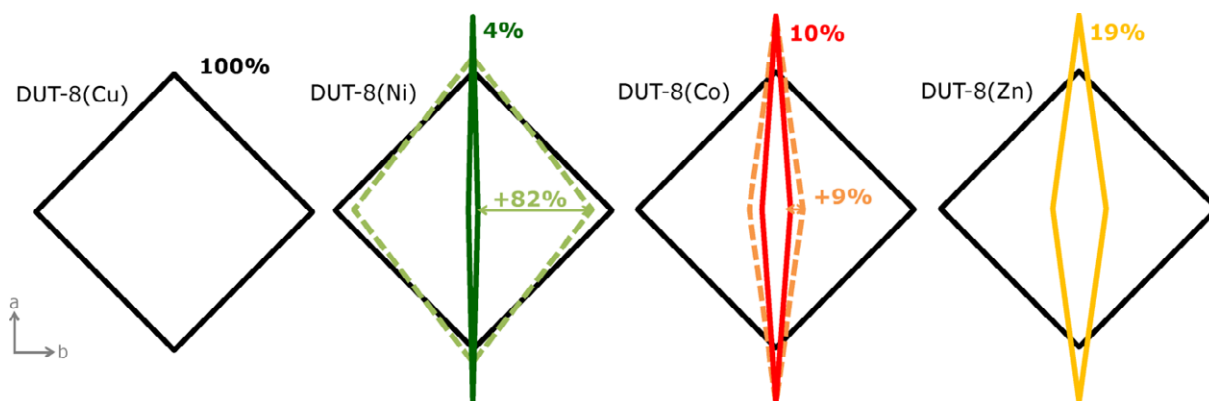

Figure S5: Schematic representation of the proposed structural flexibility of the DUT-8 series. Black solid line represents the channel along *c* of the "open state" in the "as made" material, colored solid line represents the channel of the "activated" material ("closed state") and the colored dashed line represents the channel of the "activated" material during CO_2 adsorption at p/p$_0$ 0.95 and 196 K.
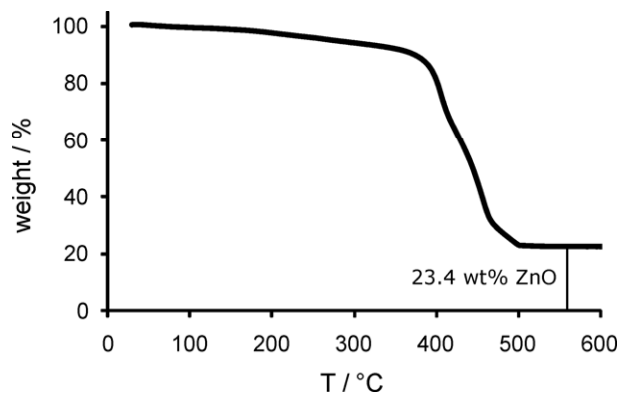
3

3. Thermogravimetric analysis (TGA)

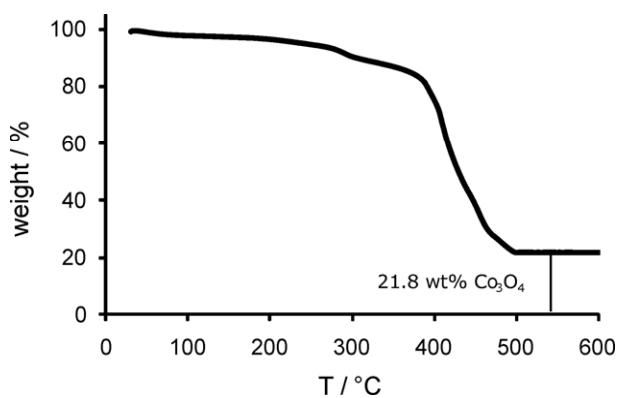Figure S6: TGA of $Zn_2(2,6\text{-ndc})_2(dabco)(DMF)_{0.2}(H_2O)_{0.5}$ (DUT-8(Zn)) in air.

Figure S7: TGA of $Co_2(2,6\text{-ndc})_2(dabco)(DEF)_{0.5}(H_2O)$ (DUT-8(Co)) in air.
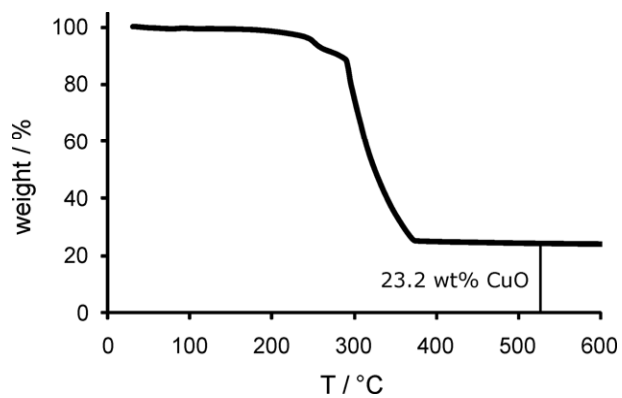

Figure S8: TGA of $Cu_2(2,6\text{-ndc})_2(dabco)(H_2O)$ (DUT-8(Cu)) in air.
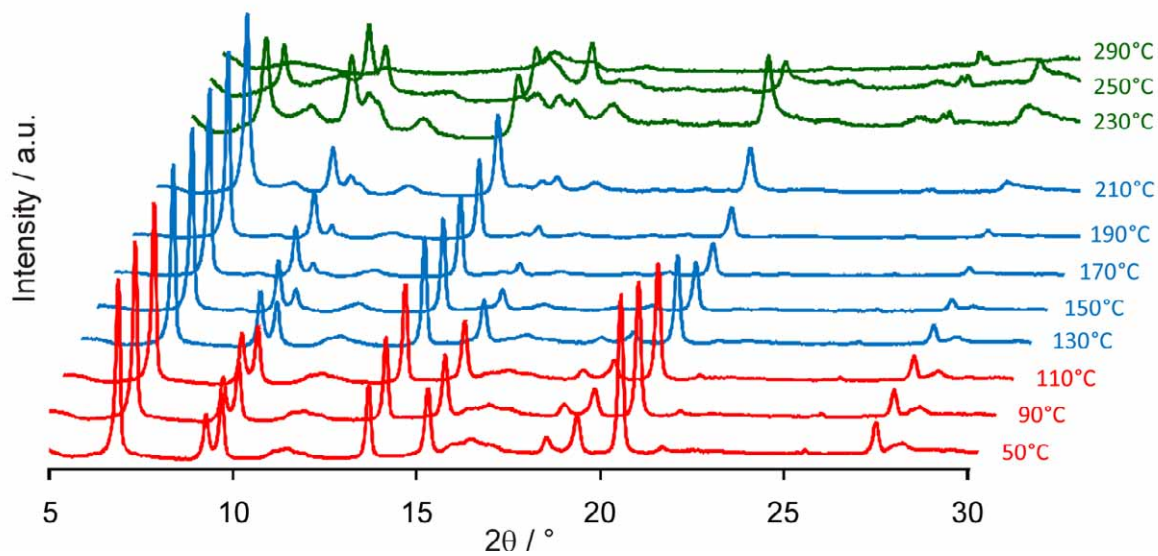
4

4. Thermodiffraction

Figure S9: Thermodiffraction of DUT-8(Cu) (starting from "as made") in argon atmosphere.
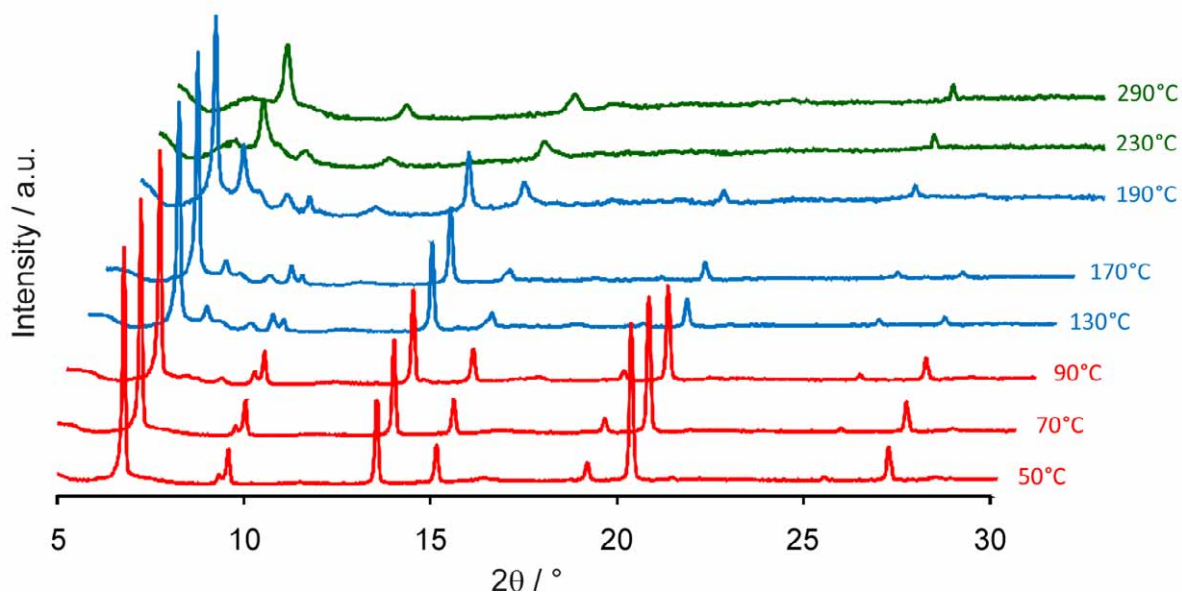

Figure S10: Thermodiffraction of (DUT-8(Co) (starting from "as made") in argon atmosphere.
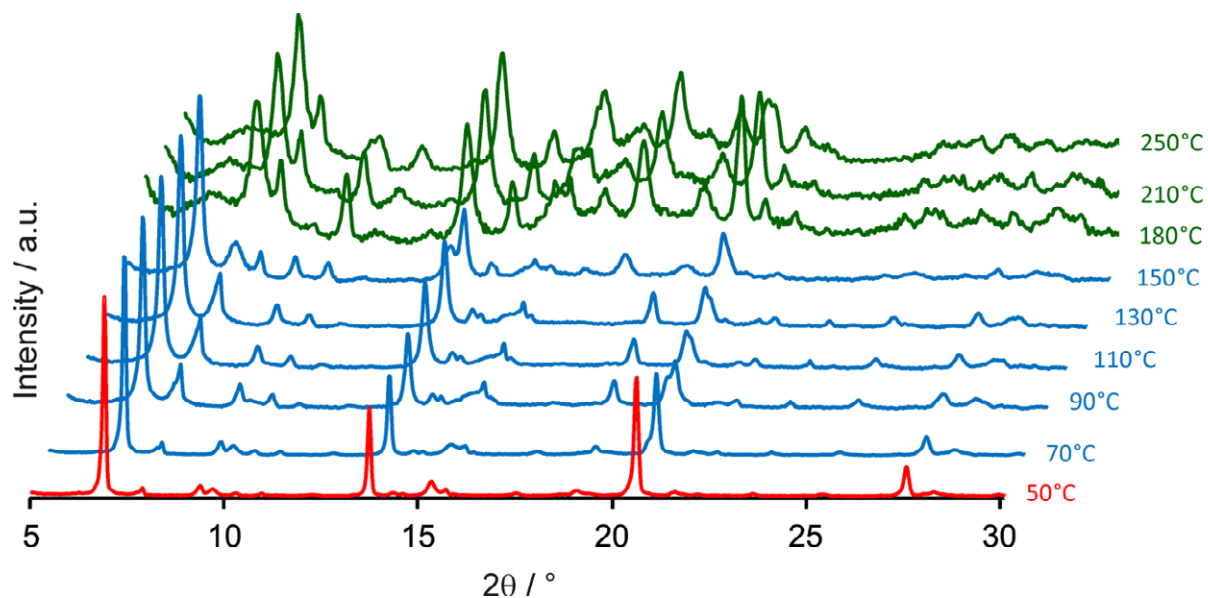
5

Figure S11: Thermodiffraction of DUT-8(Zn) (starting from "as made") in argon atmosphere.
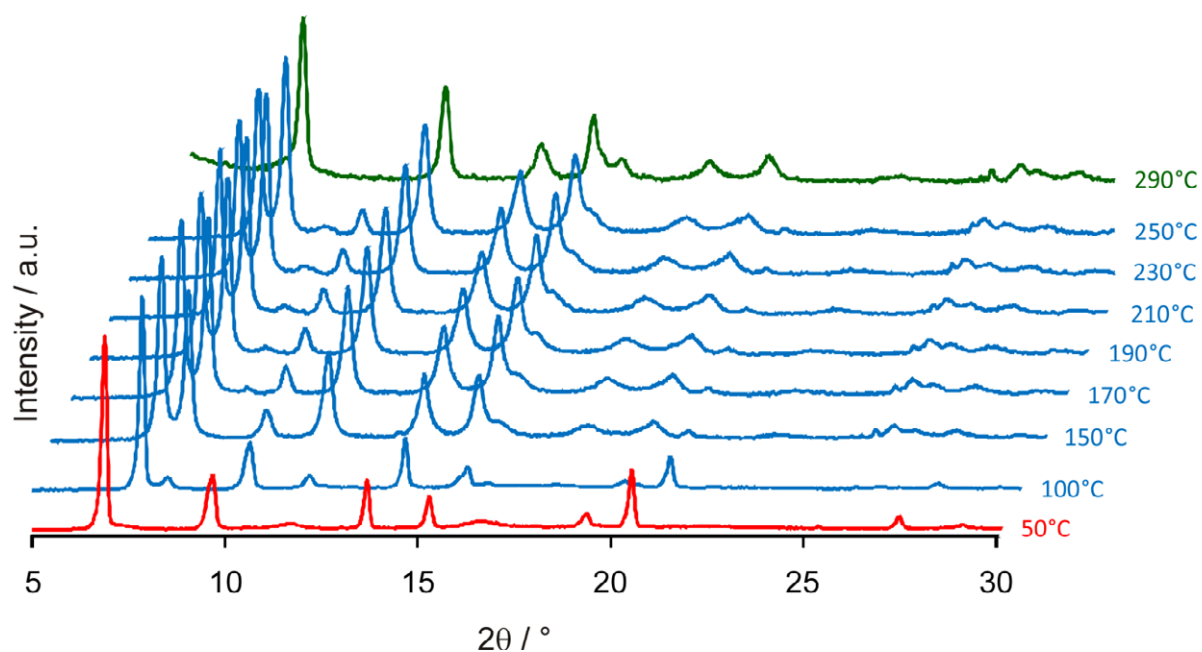

Figure S12: Thermodiffraction of DUT-8(Ni) (starting from "as made") in argon atmosphere.
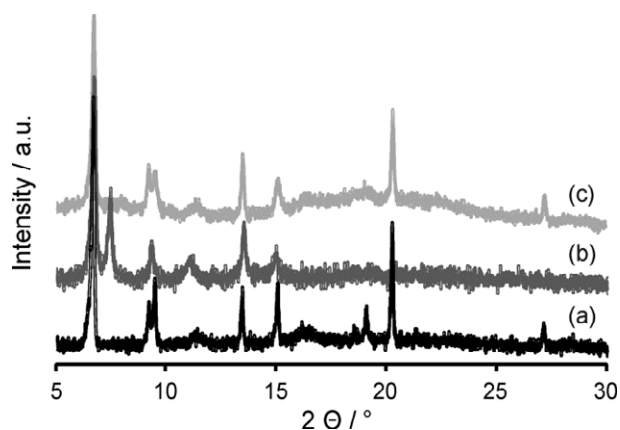
6

5. Powder X-ray diffraction pattern

Figure S13: PXRD of DUT-8(Co) as made (a), activated at 373K in vacuum (b) and resolvated in DMF (c).
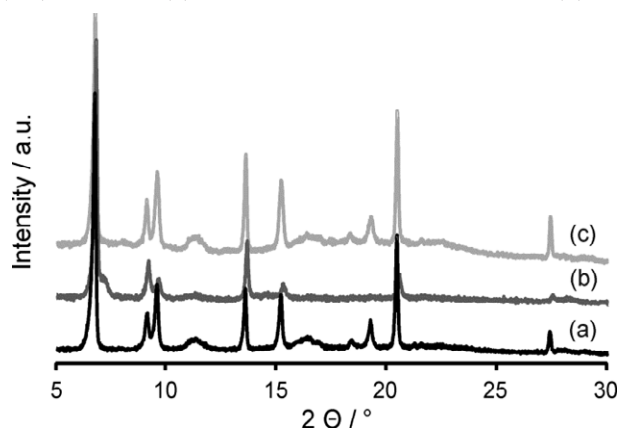
Figure S14: PXRD of DUT-8(Cu) as made (a), activated at 393K in vacuum (b) and resolvated in DMF (c).
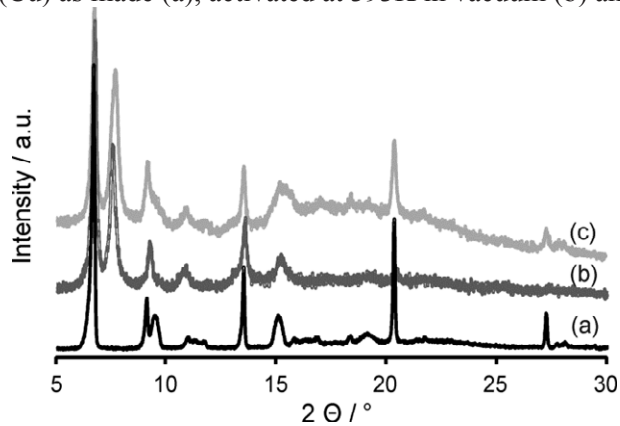
Figure S15: PXRD of DUT-8(Zn) as made (a), activated at 353K in vacuum (b) and resolvated in DMF (c).
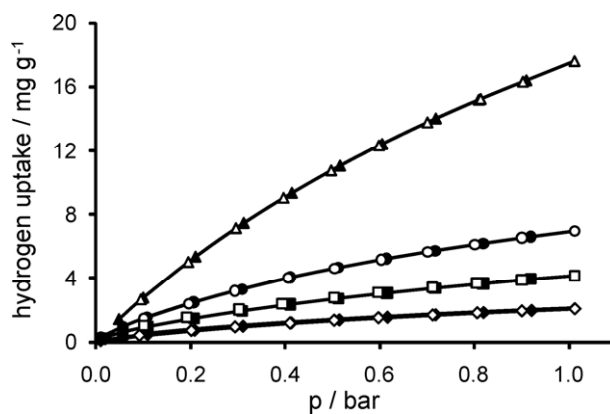
6. Adsorption

Figure S16: Low pressure hydrogen (77 K) adsorption (filled symbols) and desorption (empty symbols) isotherm of DUT-8(Zn) (squares), DUT-8(Co) (circles), DUT-8(Cu) (triangles), DUT-8(Ni) (diamonds).

The storage capacity at 77 K and 1 bar for DUT-8(Cu) is 17.62 mg g^{-1}, for DUT-8(Co) 6.98 mg g^{-1}, for DUT-8(Zn) 4.17 mg g^{-1} and for DUT-8(Ni) 2.11 mg g^{-1}.
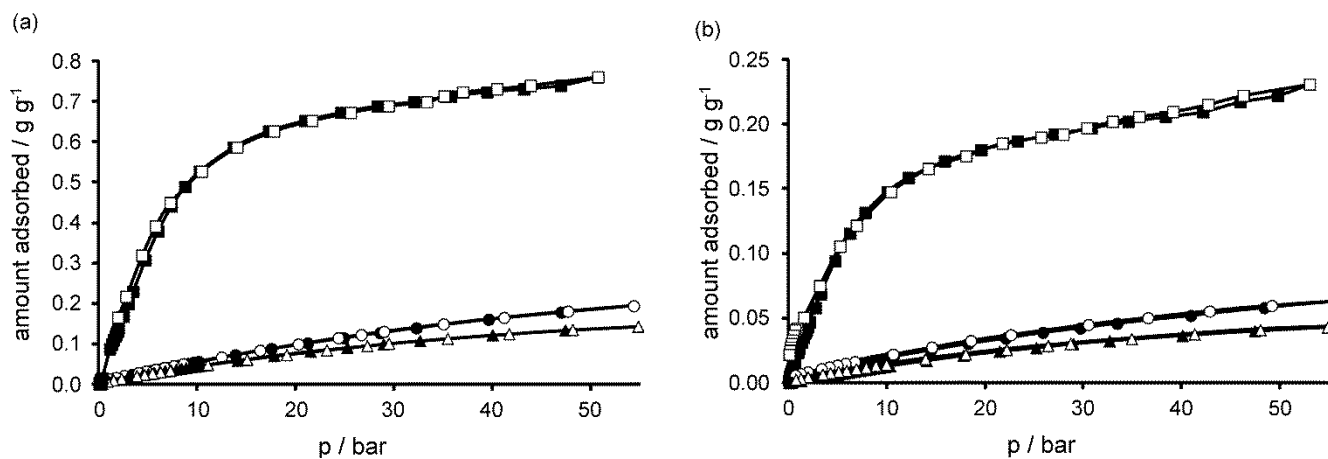

Figure S17: High pressure CO_2 (squares), O_2 (circles) and N_2 (triangles) adsorption (filled symbols) and desorption (empty symbols) isotherms of (a) DUT-8(Cu) and (b) DUT-8(Zn) at 298 K.
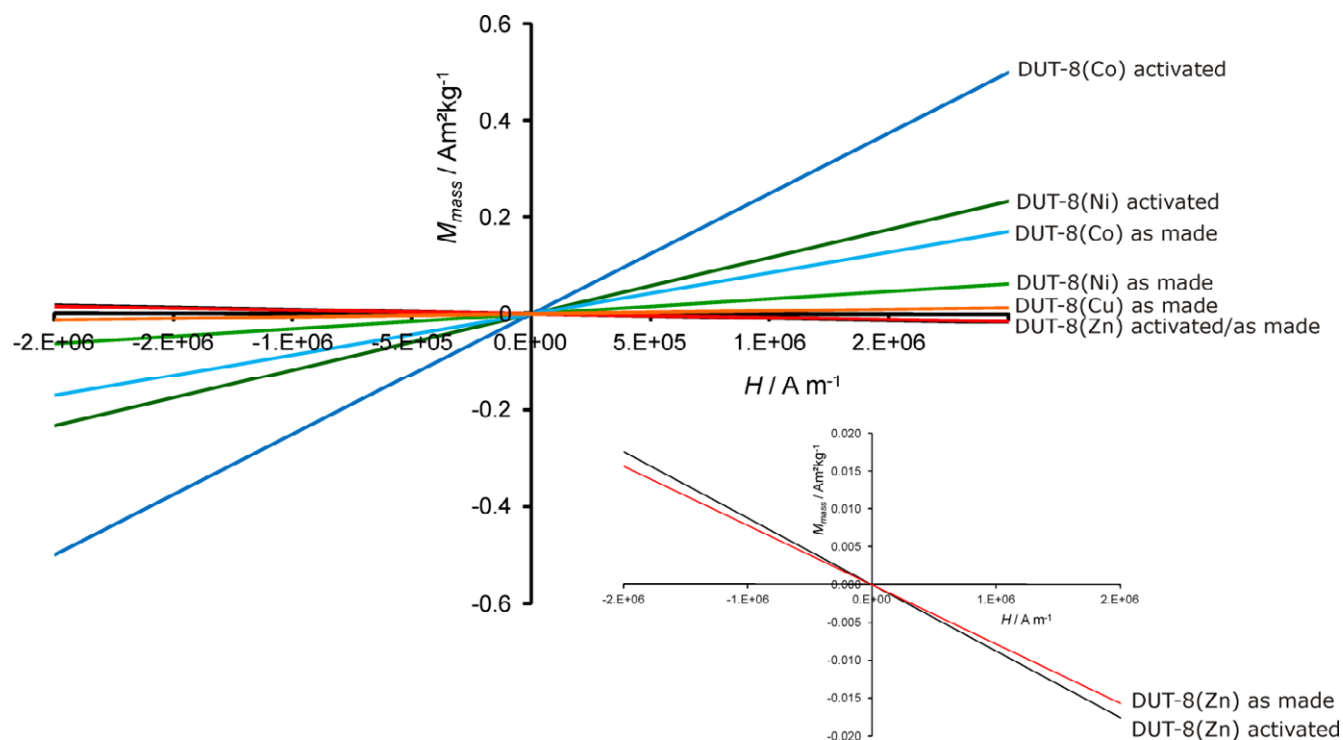
7. Magnetisation measurements

Figure S18: Magnetization curves of DUT-8(Co) (blue and light blue), DUT-8(Ni) (green and light green), DUT-8(Cu) (orange) and DUT-8(Zn) (red and black) in a magnetic field of ±3 T (~2,4 MA m^{-1}), inset: Magnetization curves of DUT-8(Zn) (red and black).

Magnetisation measurements of activated and solvent loaded samples were performed on a PPMS-VSM vibrating sample magnetometer by Quantum Design. The magnetisation data were recorded in a field range of ±3 T (~2.4 MA m^{-1}) at 300 K with a field ramp of approx. 200 Oe s^{-1} (~15.9 kA(ms)$^{-1}$). About 10 mg of the powdered sample were therefore sealed in a gelatine capsule (size 4) using a two-component adhesive. For data collection the capsule was fixed in a tube and mounted on the instrument sample holder.

The magnetization curves (mass magnetization M_{mass} vs. applied magnetic field H) (Fig. S18) show paramagnetic behaviour for the cobalt, nickel, zinc and copper containing DUT-8 phases. In contrast the zinc containing compound shows diamagnetic behaviour. According to the linear dependency of s on H a linear regression was used to calculate the magnetic mass susceptibilities, giving values of $\chi_{mass} = 11.76 \cdot 10^{-8}$ m^{3}kg^{-1} and $\chi_{mass} = 3.06 \cdot 10^{-8}$ m^{3}kg^{-1} for the activated and "as made" DUT-8(Ni) phase, $\chi_{mass} = 24.96 \cdot 10^{-8}$ m^{3}kg^{-1} and $8.47 \cdot 10^{-8}$ m^{3}kg^{-1} for the activated and "as made" DUT-8(Co) phase, $\chi_{mass} = 0.59 \cdot 10^{-8}$ m^{3}kg^{-1} the activated DUT-8(Cu) phase and $\chi_{mass} = -0.88 \cdot 10^{-8}$ m^{3}kg^{-1} and $-0.78 \cdot 10^{-8}$ m^{3}kg^{-1} for the activated and "as made" DUT-8(Zn) phase, respectively.

The paramagnetic susceptibilities χ within the activated phases of the DUT-8-family follow the order:

$\chi_{DUT-8(Cu)} < \chi_{DUT-8(Ni)} < \chi_{DUT-8(Co)}$

8. ^{129}Xe-NMR
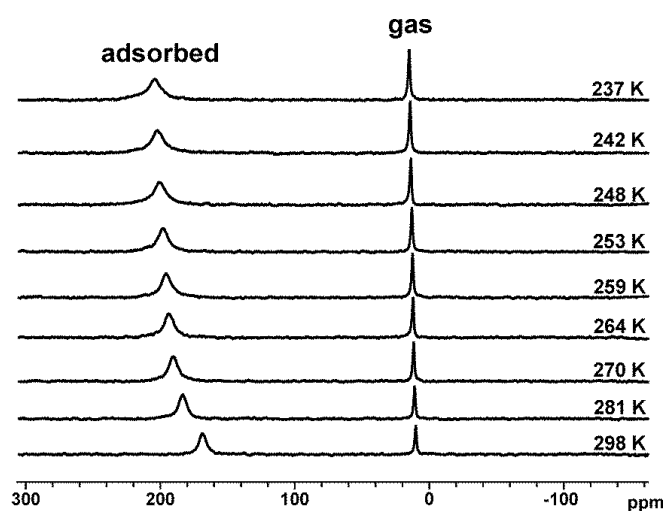

Figure S19: Temperature-dependence of the ^{129}Xe NMR spectra of xenon adsorbed on DUT-8(Cu) at constant pressure of 15 bar.
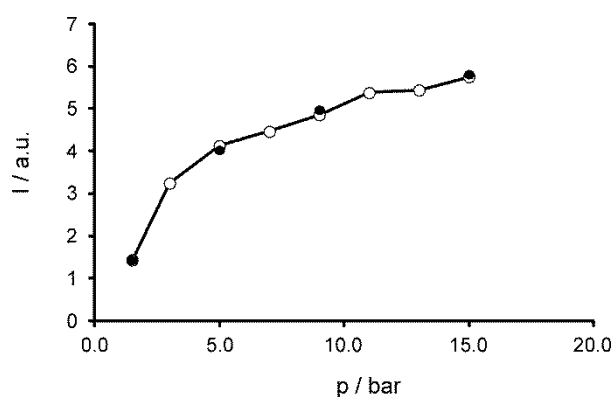

Figure S20: Intensity of the signal due to adsorbed xenon in DUT-8(Cu) determined from the spectra shown in Figure 9. Adsorption: filled circles, desorption: open circles. The lines are drawn to guide the eye.
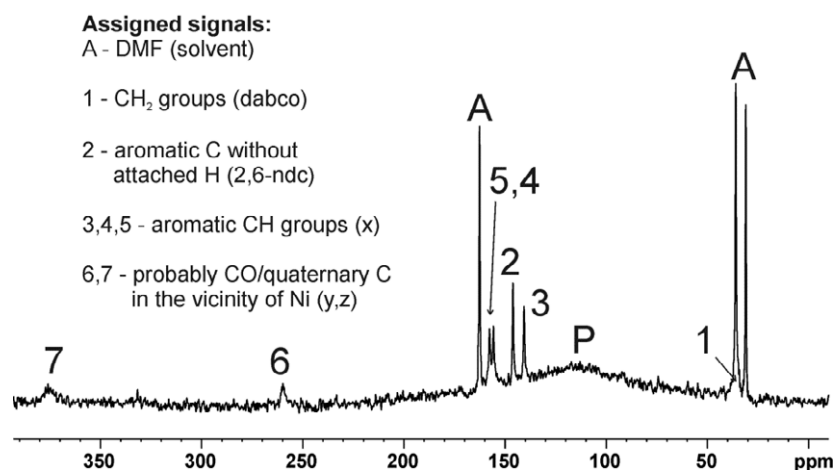
9. ^{13}C MAS NMR

Figure S21: Directly excited ^{13}C MAS NMR spectrum of DUT-8(Ni) measured at room temperature with a sample spinning rate of 14 kHz. P denotes the broad signal caused by the probe and is not due to the MOF.